separations

MDPI

Article

Degradation of Azo Dye by Ultrasound in Rotating Flow Field

Chunwei Shi [1,*], Fan Yang [1] and Xiaogang Qu [2]

[1] School of Petroleum and Chemical Engineering, Liaoning Petrochmical University, Fushun 113001, China
[2] Fushun Special Steel Co., Ltd., Fushun 113001, China
* Correspondence: chunweishilnpu@126.com

Abstract: Azo dyes such as Congo red can easily cause cancer when they come into contact or are absorbed by the human body, so it is urgent to find a fast and simple method for degrading Congo red. In order to better achieve this research goal, an ultrasonic method was used to degrade Congo red solution in a rotating flow field. The concentration of hydroxyl radical in the solution was significantly increased under the action of ultrasonic cavitation, chemical action of zero valent iron, and mechanochemistry. Under the strong oxidation of hydroxyl radical and the reduction of nano zero valent iron peeled off in the reaction process, the reaction speed is significantly accelerated and should promote the reaction. The effect of increasing stirring and adding iron powder particles on ultrasonic cavitation was studied by numerical simulation, and the yield of hydroxyl radical in the system was measured by fluorescence analysis. The experimental results show that, first, the rotating field formed by mixing increases the uniformity of ultrasonic sound field distribution and the amplitude of sound pressure, and it improves the cavitation intensity. In the effective dispersion area, the strong ultrasonic wave can form a temporary high-energy microenvironment in the suspension through cavitation, generate high strength shockwaves and micro jets, and thus significantly deagglomerate the iron powder aggregates. The addition of iron powder particles then provides a complementary Fenton reagent for the degradation reaction. The concentration of hydroxyl radicals in the solution was significantly increased by the synergy of the two actions. The degradation rate of Congo red reached more than 99% after 30 min of reaction.

Keywords: rotating flow field; ultrasonic cavitation; hydroxyl radical; azo dyes; stan

Citation: Shi, C.; Yang, F.; Qu, X. Degradation of Azo Dye by Ultrasound in Rotating Flow Field. *Separations* **2023**, *10*, 321. https://doi.org/10.3390/separations10050321

Academic Editor: Guoquan Zhang

Received: 1 April 2023
Revised: 15 May 2023
Accepted: 19 May 2023
Published: 22 May 2023

1. Introduction

Azo dyes are the most-used kind of synthetic dyes, accounting for more than 60% of the total [1]. These compounds are widely used in textile, food, cosmetics, pharmaceutical, and other industries because of their simple synthesis process, low cost and good dyeing performance [2]. Azo dyes contain at least one azo group and are often connected with aromatic rings [3]. Because dye wastewater has the characteristics of high acidity, high chroma, and strong toxicity, it is extremely harmful to the environment [4,5], so how to effectively treat dye wastewater has been a topic of close attention.

With the development of dye production technology, it is increasingly difficult to treat dye wastewater. The traditional dye wastewater treatment method has been difficult to meet the treatment requirements of non-degradable dye wastewater [6,7]. At present, many methods have been developed in the world to treat azo dye wastewater and have achieved good results, such as the Fenton method [7–9], the catalytic oxidation method [10–12], the ozone oxidation method [13,14], the photocatalysis method [15,16], etc. Among them, the Fenton method has a good effect on the degradation of azo wastewater, but it is troublesome to supplement and recover Fenton agent.

Ultrasound has the characteristics of high frequency, short wavelength, and strong directionality. At present, ultrasonic effects have been widely applied, such as ultrasonic cleaning, ultrasonic humidifiers, ultrasonic oil removal, and medical ultrasonic examinations. In the process of chemical reactions, the cavitation effect of ultrasound can increase

the temperature of the solution, and the dissolution of solutes is accelerated through vibration instead of stirring, accelerating the chemical reaction.

As an advanced oxidation process, ultrasonic technology has been proved to be able to treat any kind of wastewater, so it is widely used to degrade organic pollutants in water. Compared to some traditional degradation methods, ultrasound technology is simpler, cleaner, and more efficient. The working mechanism of this method is that the hydroxyl radical generated by ultrasonic cavitation reacts with organic pollutants in water to achieve the degradation of organic substances. Ultrasonic cavitation refers to the collapse and rupture of cavitation bubbles driven by ultrasound. At the moment of rupture, high temperature and pressure are generated inside the bubbles, accompanied by the formation of shockwaves. At the same time, the high temperature generated by cavitation will decompose water molecules into H atoms and hydroxyl radical. In addition, the shockwave and micro jet generated by cavitation bubbles cause the oxidant to escape into the interface and aqueous solution, which will lead to rapid oxidation between the oxidant and organic pollutants in the solution [17]. Numerous experimental studies have shown that the degradation of organic pollutants by ultrasonic cavitation is influenced by various factors, including temperature, pressure, and shockwaves generated by cavitation bubbles. For a given solution, these factors are mainly influenced by the characteristics of the ultrasonic field. Chen et al.'s research shows that ultrasound intensity, ultrasound frequency, and liquid viscosity have a direct impact on the degradation rate of Congo Red [16].

The refining mechanism of spiral stirring ball milling generally applies external forces to the material to make it ultra fine. The types of external forces applied include compression, bending, shear, splitting, grinding, striking, or impact, etc. The applied external forces are very complex, and in most cases, multiple force applications exist simultaneously. According to the different ways in which external forces are applied, the ultrafine methods of materials can generally be divided into several methods, such as extrusion crushing, impact crushing, friction shear crushing, and splitting crushing. The working principles of various crushing equipment are also mainly based on these principles. The stirring ball mill mainly consists of a stationary cylinder filled with small diameter grinding balls and a rotating stirring rod. The stirring rod stirs the grinding balls to generate friction, shear, and a small amount of impact to crush materials. Unlike ordinary ball mills and vibration mills, the input power of stirred ball mills is directly used to drive the grinding balls at high speed to achieve the goal of ultra-fine materials. Therefore, the stirred ball mill is the one with the highest energy utilization rate among solid powder ultrafine equipment.

In this paper, the ultrasonic method is introduced into the rotating flow field, and sulfuric acid, iron powder, and hydrogen peroxide are used as the Fenton reagent to promote the continuous reaction between solid and liquid phases. The rotating flow field enhances the cavitation effect of ultrasound, and the addition of iron powder provides a complementary Fenton reagent for the degradation reaction. These two kinds of actions synergize to significantly increase the concentration of hydroxyl radicals in the solution, thus improving the degradation rate of ultrasonic degradation of Congo red wastewater [16,18]. The reaction equipment in this experiment is simple, easy to operate, and has good removal effect of organic substances in the actual production of wastewater [19–21], is low cost, and is convenient for industrialization.

2. Materials and Methods

2.1. Reagents and Instruments

Congo red, sulphuric acid, hydrogen peroxide (30% H_2O_2), terephthalic acid (TA), and ferrous chloride were analytically pure, and stan's diameter was 150~500 μm. The above obtained reagents are from Sinopharm Chemical Reagent Co., (Shanghai, China).

It is generated on the SB-5200DTD cleaning machine produced by Ningbo Xinyi Ultrasonic Equipment Co., Ltd. (Ningbo, China) (ultrasonic power: 300 W, ultrasonic frequency: 40 kHz). The absorbances were recorded on a ultraviolet visible spectrophotometer

(Tianjin Tuopu Instrument Co., Ltd., Tianjin, China). Fluorescence spectrums were obtained using a F-2500 fluorescence spectrophotometer, JEOL (Tokyo, Japan). XRD was recorded on a TD-3300 XRD analyzer (Bruker Beijing Technology Co., Ltd., Beijing, China).

System (I) is an ultrasonic system, without stirring and the addition of stan, with the addition of hydrogen peroxide and ferrous chloride; System (II) is an ultrasonic stirring synergistic system, without the addition of stan, and with the addition of hydrogen peroxide and ferrous chloride; and System (III) an ultrasonic stirring synergistic system with the addition of stan, sulphuric acid, and hydrogen peroxide, and without the addition of ferrous chloride.

2.2. Degradation Experiment

2.2.1. Experimental Process

The device used in the ultrasonic mixing process is shown in Figure 1. Ultrasonic assisted aqueous solution stirring in a stainless steel reactor (diameter 100 mm, height 130 mm) is used to degrade Congo red solution. Congo Red (20 mg) was added to 1500 mL of deionized water to prepare a Congo Red solution. During the experiment, the height of the stirring rod was adjusted to a distance of 5 mm from the bottom of the reaction vessel, while the average temperature of the chemical reaction in the reactor is 50 °C.

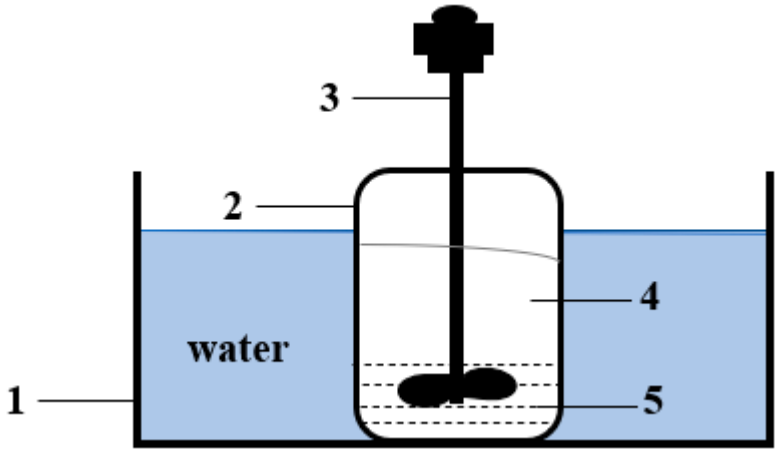

Figure 1. Ultrasonic device diagram. (1. Ultrasonic cleaner; 2. Stainless steel reactor; 3. Stirrer; 4. Reaction solution; 5. Ferrous powder).

In System (I), 2 mol/L hydrogen peroxide 100 mL and 1 mol/L ferrous chloride 200 mL were added. In System (II), the frequency of the ultrasonic generator is 28 kHz and the power is 100 W, while the speed of stirring rod is 250 r/min. A total of 2 mol/L hydrogen peroxide 100 mL and 1 mol/L ferrous chloride 200 mL were added. In System (III), the frequency of the ultrasonic generator is 28 kHz, and the power is 100 W and the speed of the stirring rod is 250 r/min. A total of 500 g stan, 2 mol/L sulphuric acid 50 mL, and 2 mol/L hydrogen peroxide were added. Sampling and centrifugation for testing took place every 10 min.

2.2.2. Characterization Method of Degradation Rate

The solution was taken every 10 min during the reaction process, and its absorbance was measured with a ultraviolet visible spectrophotometer (UV-2500). The scanning range of the ultraviolet spectrophotometer was 200~2500 nm, and the degradation rate was used for the degradation effect η, as shown in Formula (1):

$$\eta = \frac{n_0 - n_t}{n_0} \times 100\% \quad (1)$$

where n_0 is the amount of CR before degradation (mmol), and n_t is the amount of CR after degradation (mmol).

2.2.3. Detection Method of Hydroxyl Radical

Detection of hydroxyl radicals was achieved by fluorescence spectrometry with TA as the capture agent. A total of 10 mL of solution was extracted from the set time using a disposable pipette and an equal amount of capture agent and buffer were added to the system. A sample was taken and the filtered solution was then placed in a brown glass bottle. After sampling and dilution at different reaction times, the fluorescence intensity of 2-hydroxyterephthalic acid was measured by fluorescence spectrometer. The fluorescence intensity was proportional to the concentration of hydroxyl radical. The excitation wavelength is 315 nm, the receiving wavelength range is 360~600 nm, and the scanning interval is 5 nm.

3. Numerical Simulation

It is a common method to change the turbulence intensity distribution by introducing a ultrasonic field in the current scientific research field. The pressure change of the sound pressure in the ultrasonic field is used to change the pressure field inside the fluid, which brings about the disturbance of the flow field and, at the same time, increases the cavitation phenomenon inside the turbulence, thus changing the turbulence intensity distribution. Although the introduction of ultrasonic field pressure field will change the distribution of turbulence intensity, it will bring negative effects to the gas-liquid solid three-phase abrasive flow polishing process when the ultrasonic cavitation control method is unreasonable. Therefore, it is necessary to study ultrasound fields with different amplitudes and frequencies, and obtain the optimal parameters through comparative analysis.

3.1. Establishment of Model

It is assumed that the fluid in the stainless steel reactor is an ideal incompressible fluid, which belongs to the turbulent field. The finite volume method is selected to calculate the flow field using the SIMPLE algorithm of unstructured mesh. The continuous equation is:

$$\frac{\partial \rho}{\partial t} + \frac{\partial (u_\rho)}{\partial x} = 0 \tag{2}$$

where ρ is fluid density, g/cm^3; u is relative velocity of fluid, m/s; and t is time, s.

Because the multiphase flow model is needed to simulate the flow of solid–liquid two-phase mixed fluid, the Eulerian model is selected for this simulation. Equations (3)–(5) are used to calculate the sound field distribution, and the influence of background velocity and pressure on the sound propagation is considered.

$$\frac{\partial \rho'}{\partial t} + (V_0 \cdot \nabla)\rho' + (V \cdot \nabla)\rho_0 + \rho'(\nabla \cdot V_0) + \rho_0(\nabla \cdot V) = 0 \tag{3}$$

$$\frac{\partial V}{\partial t} + (V_0 \cdot \nabla)V + (V \cdot \nabla)V_0 + \frac{1}{\rho_0}\nabla p_\mathrm{a} - \frac{\rho'}{\rho_0^2}\nabla p_0 = 0 \tag{4}$$

$$\rho = p_\mathrm{a}/c_0^2 \tag{5}$$

where p_0 = 1 atm (1.0 × 105 Pa) is static pressure of medium, ρ is fluid density, p is sound pressure, u is particle velocity, and c_0 is sound velocity.

3.2. Sound Field Analysis

Sound field distribution is an important factor affecting ultrasonic degradation [22]. In this paper, COMSOL Multiphysics finite element analysis software is used to carry out numerical research on the device model in Figure 1. This software is based on the finite element method and achieves coupling of multiple physical fields by solving partial differential equations. The entire simulation process is divided into two steps. Firstly, simulate the flow field caused by stirring in the two-phase flow module. Secondly, the simulated velocity and pressure are substituted into the background velocity and pressure

in the convection wave equation module as the velocity and pressure of the medium in the acoustic wave propagation process, and then the acoustic field distribution in the water tank is obtained. We analyzed the sound field distribution under different stirring speeds.

When the stirring speed is 0 r/min, the sound wave propagates upward from the bottom of the tank and finally forms a standing wave sound field after continuous reflection (Figure 2a). The literature [23] reported that the standing wave acoustic field will reduce the uniformity of the acoustic field and reduce the efficiency of the sonochemical reaction. Therefore, it is speculated that the degradation rate of the system without stirring will be relatively low.

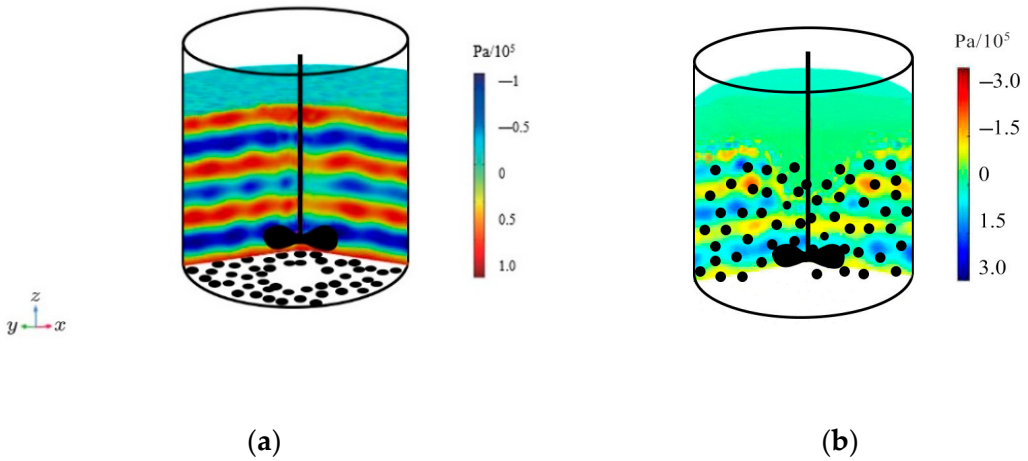

Figure 2. Sound field distribution at different stirring speeds. Black dots represent stan. (**a**) 0 r/min; (**b**) 500 r/min.

In the process of spiral stirring ball milling, the force on each contact point of material particles in the grinding cylinder is unequal, that is, the stress intensity of the grinding ball at any position in the grinding cylinder is different. At the radial position, the linear velocity of grinding balls on different radii is not equal. From the stirring shaft to the top of the thread, the linear velocity increases linearly, reaching its maximum at the top of the stirring rod thread. From the top of the stirring rod thread to the annular crushing area of the cylinder wall, the linear velocity then gradually decreases. In the axial position, due to the unequal force exerted on the grinding ball, the linear velocity of the grinding ball varies between layers, resulting in a velocity gradient. Therefore, friction and shear forces exist during the spiral stirring ball milling process. From the above analysis, it can be seen that the refining effect of the spiral stirring ball milling method on iron powder is mainly achieved through the impact crushing effect of the grinding ball on the powder and the friction and shear effect caused by the speed difference between the grinding balls on the powder.

When the stirring speed reaches 500 r/min, the standing wave field has been weakened and the sound field becomes more uniform than that without stirring (Figure 2b). The amplitude of sound pressure has increased more than three times. It shows that mechanical stirring can eliminate the standing wave sound field, which is caused by the rotating flow caused by stirring.

Therefore, adding stirring in the ultrasonic wave is beneficial to improve the cavitation intensity and is expected to improve the degradation rate of Congo Red in the degradation experiment.

4. Results and Discussion

In order to verify the correctness of numerical calculations, this paper designed an ultrasound assisted mechanical stirring experiment to measure the degradation rate of Congo Red solution.

4.1. Determination of Hydroxyl Radical

Using terephthalic acid as the capture agent of hydroxyl radical, fluorescence spectrometry was used for detection [24,25]. Figure 3 shows the fluorescence spectra of terephthalic acid solution in the ultrasonic system (I), the ultrasonic stirring synergetic system (II), and the synergetic system with iron powder (III) at different times.

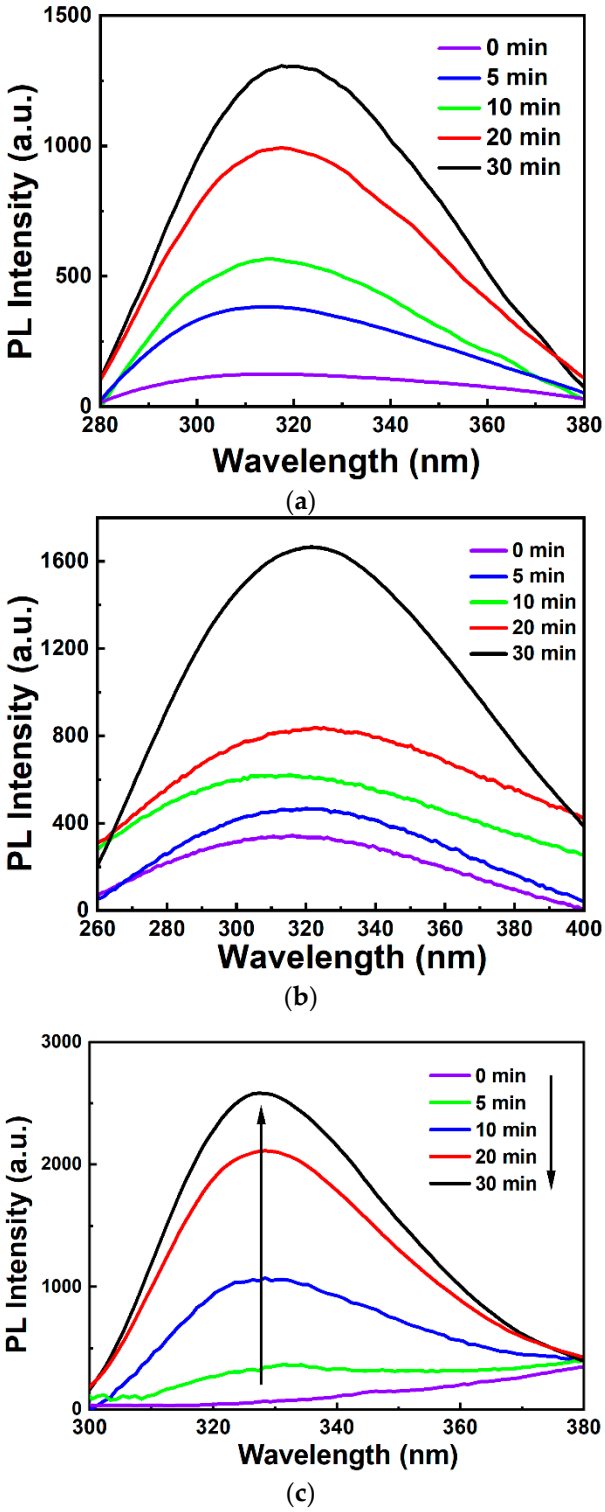

Figure 3. Fluorescence spectra of three systems at different times. (**a**) System (I); (**b**) System (II); (**c**) System (III).

It is shown that the fluorescence intensity of the solution in the three systems increases with the reaction time. The fluorescence intensity of system III is 20% higher than that of system II and 55% higher than that of system I, indicating that the addition of iron powder and stirring is beneficial to the production of more hydroxyl radicals in the system. The reaction equations are as follows [26,27]:

$$Fe^0 + H_2SO_4 = Fe^{2+} + SO_4{}^{2-} + H_2 \quad (6)$$

$$Fe^{2+} + H_2O_2 \rightarrow Fe^{3+} + \cdot OH + OH^- \quad (7)$$

$$2Fe^{3+} + Fe^0 \rightarrow 3Fe^{2+} \quad (8)$$

$$2H_2O_2 \rightarrow 2H_2O + O_2 \quad (9)$$

$$5Fe^0 + H_2O + 3O_2 \rightarrow Fe_2O_3 + Fe_3O_4 + H_2 \quad (10)$$

$$Fe^{3+} + 3H_2O \rightarrow Fe(OH)_3 + 3H^+ \quad (11)$$

$$2Fe(OH)_3 + Fe^{2+} \rightarrow Fe_3O_4 + 2H_2O + 2H^+ \quad (12)$$

$$Fe_2O_3 + H_2O \rightarrow 2FeOOH \quad (13)$$

$$2FeOOH + Fe^{2+} \rightarrow Fe_3O_4 + 2H^+ \quad (14)$$

From the above reaction, it can be seen that ultrasound (less than 100 kHz) can generate a very large fluid shear force between the iron powder coupled with the impact force, so that a new reaction layer will be generated in the iron powder cortex, thus promoting the oxidation of the hydroxyl radical generated by the reaction. On the other hand, under the presence of the ultrasound, zero valent iron can also form Fe^{2+}, and a Fenton -ike reaction occurs between Fe^{2+} and H_2O_2, increasing the reaction rate. Under the condition of ultrasonic ball milling, with the increase in time, the peak strength increases continuously, indicating that the number of hydroxyl radicals increases continuously, which is significantly more than the number of hydroxyl radical produced in the process of ball milling and ultrasonic alone. The degradation efficiency of Congo red gradually decreases with the increase in the initial concentration of reactants due to the low frequency and low sound intensity of the ultrasonic generator itself, which makes it difficult to generate enough ·OH radicals to participate in the oxidation reaction during the ultrasonic cavitation process.

The surface of the used iron powder contains a certain proportion of iron tetroxide and iron oxide. However, under the synergistic effect of ultrasound and stirring, the oxide will have a certain degree of detachment, so the degradation effect will be relatively stable.

As the initial concentration increases, the probability of reactants participating in the reaction increases, and the reaction proceeds in a positive direction, but it is not entirely proportional. In cases where the concentration of reactants is too high, azo dye molecules will compete for reaction sites on the surface of zero valent iron, leading to a decrease in reaction rate and a hindered reaction process.

4.2. Detection and Analysis of Reaction Sediment

The unreacted iron powder and the precipitate filtered and dried from the solution after 30 min of reaction are, respectively, tested by XRD (Figure 4).

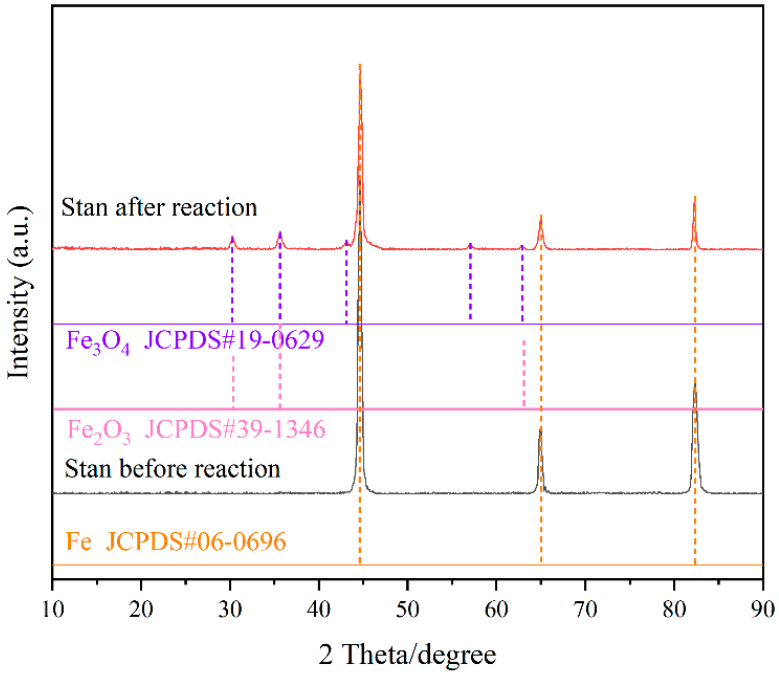

Figure 4. XRD patterns of stan before and after reaction.

The results show that the iron powder before the reaction has strong characteristic diffraction peaks at 44.67°, 65.02° and 82.33°. The characteristic diffraction peak intensity of Fe^0 in the precipitate after reaction is significantly reduced, while the characteristic diffraction peaks of Fe_3O_4 and Fe_2O_3 appear [28]. This result helps to verify the existence of the hydroxyl radical generation reaction (6)~(14).

4.3. Degradation of Congo Red

Congo red degradation reaction experiments were conducted on three systems and compared system I (without ultrasound in system I) and compared system II (without stirring in system III), as shown in Figure 5. The degradation rate of system (I) is 45%, and after adding stirring, the degradation rate of system (II) increases to 70%. This indicates that the synergistic system of ultrasound and stirring is beneficial for improving the degradation rate. In system (III), ferrous chloride was replaced by stan and sulfuric acid, and the degradation rate was further improved, indicating that stan and sulfuric acid was more conducive to the formation of hydroxyl radical. The degradation rate of compared system I was lower than that of system I, indicating that the contribution of ultrasound to hydroxyl radical was higher than that of stirring. The degradation effect of comparison system II is between system II and system III, which indicates that for this experiment, the contribution of iron powder and sulfuric acid to hydroxyl radical is higher than that of stirring.

According to the Bessel standard deviation formula, after 30 min of reaction, the standard deviation is 30, which is a large value, indicating that different systems have a significant impact on the degradation rate of Congo Red. It shows that system (III) has high degradation activity, and the degradation rate is directly proportional to the amount of hydroxyl radicals generated.

4.4. Mechanism Discussion

When using ultrasound to treat iron powder materials, there are a large number of micro bubbles at the internal microcracks and solid-liquid interfaces of the iron powder particles. Strong ultrasound can easily cause cavitation in the liquid near iron powder particles, forming a large number of cavitation bubbles. These cavitation bubbles collapse under the alternating sound pressure of ultrasound, generating extremely high pressure,

forming shockwaves or micro jets, and thereby exerting significant impact crushing effects on the particles. Due to the collapse of cavitation bubbles, a pressure of up to 980 a t m can be generated, which is sufficient to overcome the disadvantage of the spiral stirring ball milling method that cannot crush iron powder to below 2 um due to the increase in powder strength, thereby playing a very significant refining role in the iron powder.

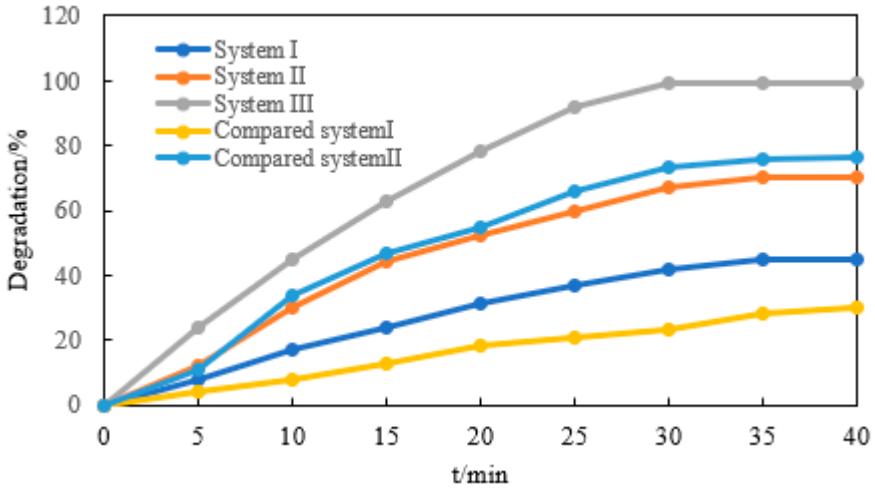

Figure 5. Effect of three systems on degradation rate of Congo red at different time.

The ball milling stirring is driven by a stirring rod to stir the mixed suspension, causing the internal parts of the mixed suspension to be stirred. The iron powder aggregates in the suspension are evenly separated and dispersed by impacts, shear, compression, and other effects. This form is very effective in promoting the circulating flow of mixed suspensions, which can significantly increase the probability of iron powder aggregates entering the effective area where dispersion can occur. Strong ultrasound has the characteristics of wave length, approximate linear propagation, and easy energy concentration. When the suspension of iron powder aggregates is directly placed in a strong ultrasound field under the action of alternating sound pressure of strong ultrasound, the micro bubbles inside the suspension undergo cavitation, and the bubbles rapidly expand. When they reach a considerable size, they quickly close and collapse. This situation generates local high temperature and high pressure, forming high-strength shockwaves and micro jets, which have a significant impact on the iron powder aggregates. This is enough to overcome the force between the nanoparticles in the aggregates, thus enabling the nanoparticles to be evenly dispersed in the liquid.

The combination of strong ultrasonic/ball milling stirring combines the advantages of ball milling stirring and strong ultrasonic, which drives the iron powder aggregates in the suspension to circulate into the effective dispersion area through ball milling stirring. In the effective dispersion area, the strong ultrasonic wave can form a temporary high-energy microenvironment in the suspension through cavitation, generate high strength shockwaves and micro jets, and thus significantly deagglomerate the iron powder aggregates.

The azo dye molecules contact with iron powder and react with hydroxyl radicals to produce Fe_3O_4 and Fe_2O_3, which are precipitated on the surface of iron powder. Next, the sediment on the surface layer is peeled off to form a new reaction layer through the mechanical action of ultrasonic, stirring, and friction. The new reaction layer continues to react, and the reaction cycle continues. The Fe^{2+} generated in the reaction will undergo Fenton reaction with the H_2O_2 generated under the action of ultrasonic cavitation, and the hydroxyl radical generated will promote the reaction in the positive direction. In addition, a certain amount of zero valent iron will also peel off during the collision of iron powder, which has a larger specific surface area and a faster reaction rate when participating in the reaction, thus promoting the progress of the reaction, as shown in Figure 6.

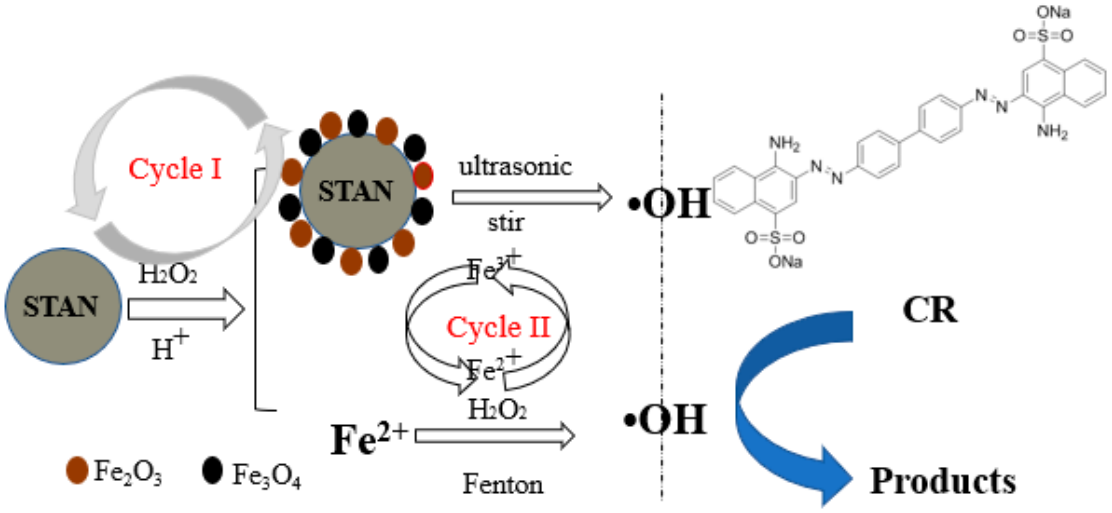

Figure 6. Mechanism diagram of degradation of CR by ultrasound and iron powder in rotating fluid.

5. Conclusions

This article proposes a method for the impact of near wall cavitation on the fragmentation of fine particles in a rotating flow field. The rotating flow field created by mechanical stirring effectively eliminates the standing wave sound field of ultrasound, and a simulation analysis is conducted on the influence of mechanical stirring on the intensity of acoustic cavitation from the perspective of sound field distribution. The synergistic system of ultrasound and mechanical stirring can effectively degrade azo dyes in water, with low raw material cost and no need to frequently supplement ferrous chloride solution. The experimental results showed that the degradation rate of Congo red reached over 99% after 30 min of reaction. This study provides a new method for the ultrasonic degradation of organic solutions, and provides important engineering guidance for the widespread application of the ultrasonic cavitation effect in industrial production of fine particle crushing.

Author Contributions: Conceptualization, C.S., F.Y. and X.Q.; analysis, C.S. and X.Q. All authors have read and agreed to the published version of the manuscript.

Funding: This research was funded by [Natural Science Foundation of Liaoning Province], grant number [2019-ZD-0055], Fushun elite youth top talent project [FSYC202007001] and [Department of Education of Liaoning Province (Liaoning Provincial Education Department)] grant number [L2020010].

Data Availability Statement: The data are not publicly available due to the organizer of Fushun elite youth top talent project who does not agree to make it public.

Conflicts of Interest: The authors declare no conflict of interest.

References

1. Benkhaya, S.; M'Rabet, S.; El Harfi, A. Classifications, properties, recent synthesis and applications of azo dyes. *Heliyon* **2020**, *11*, 3271–3282. [CrossRef]
2. Kang, C.; Ma, H.; Li, S. Fe-doped g-C3N4 photocatalytic activation of persulfate for degradation of azo dyes. *J. Liaoning Petrochem. Univ.* **2022**, *42*, 13–17.
3. Cai, M.; Su, J.; Lian, G. Sono-advanced Fenton decolorization of azo dye orange G: Analysis of synergistic effect and mechanisms. *Ultrason. Sonochemistry* **2016**, *31*, 193–200. [CrossRef]
4. Kodavatigantis, S.; Bhat, A.; Gogate, P. Intensified degradation of acid violet 7 dye using ultrasound combined with hydrogen peroxide, Fenton, and persulfate. *Sep. Purif. Technol.* **2021**, *198*, 119673–119782. [CrossRef]
5. Dailin, D.; Nordin, N.; Tan, L. State of the art bioremediation of textile dye in wastewater. *Biosci. Res.* **2022**, *19*, 914–924.
6. Liu, J.; Bao, X.; Kolesnik, I.; Jia, B.; Yu, Z.; Xing, C.; Huang, J.; Gu, T.; Shao, X.; Kletskov, A.; et al. Enhancing the in vivo stability of polycation gene carriers by using PEGylated hyaluronic acid as a shielding system. *BIO Integr.* **2022**, *3*, 103–111. [CrossRef]

7. Chen, Z.; Huang, P. Introducing a new journal: BIO Integration. *BIO Integr.* **2020**, *1*, 1. [CrossRef]
8. Saw, P.E.; Jiang, S. The Significance of Interdisciplinary Integration in Academic Research and Application. *BIO Integr.* **2020**, *1*, 2–5. [CrossRef]
9. Yang, Q.; Qi, R.; Cai, J.; Kang, X.; Sun, S.; Xiao, H.; Jing, X.; Li, W.; Wang, Z. Biodegradable polymer-platinum drug conjugates to overcome platinum drug resistance. *RSC Adv.* **2015**, *5*, 83343–83349. [CrossRef]
10. Bai, Y.; Ahmad, D.; Wang, T.; Cui, G.; Li, W. Research Advances in the Use of Histone Deacetylase Inhibitors for Epigenetic Targeting of Cancer. *Curr. Top. Med. Chem.* **2019**, *19*, 995–1004. [CrossRef]
11. Yu, Y.; Tan, K.; Shaharuddin, B.; Guo, Z.; Tan, J.J. Modelling Atrial Arrhythmia In vitro Using Pluripotent Stem Cell-derived Atrial Cardiomyocytes in Three-dimensional Culture. *BIO Integr.* **2020**, *1*, 92–94. [CrossRef]
12. Zhao, D.; Gui, G.G.; Li, Z. Application of LDHs with photocatalytic properties in water pollution treatment. *J. Petrochem. Univ.* **2022**, *35*, 36–42.
13. Benlt, H.; Bahtiyari, M. Combination of ozone and ultrasound in pretreatment of cotton fabrics prior to natural dyeing. *J. Clean. Prod.* **2015**, *89*, 116–124. [CrossRef]
14. Tezcanlt, G.; Ince, N. Individual and combined effects of ultrasound, ozone and UV irradiation. *Ultrason. Sonochemistry* **2004**, *42*, 603–609. [CrossRef] [PubMed]
15. Kumar, R.; Kumar, G.; Akhtar, M.; Umar, A. Sonophotocatalytic degradation of methyl orange using ZnO nano-aggregates. *J. Alloys Compd.* **2015**, *629*, 167–172. [CrossRef]
16. Chen, D.; Ai, S.; Liang, Z.; Wei, F. Preparation and photocatalytic properties of zinc oxide nanoparticles by microwave-assisted ball milling. *Ceram. Int.* **2016**, *42*, 3692–3696. [CrossRef]
17. Liu, J.-H.; Shen, Z.-Z.; Lin, S.-Y. Effect of mechanical agitation on ultrasonic cavitation dynamics. *Acta Phys. Sin.* **2021**, *70*, 224301–224310. [CrossRef]
18. Chen, D.; Li, D.-Y.; Zhang, Y.-Z.; Kang, Z.-T. Preparation of magnesium ferrite nanoparticles by ultrasonic wave-assisted aqueous solution ball milling. *Ultrason. Sonochemistry* **2013**, *20*, 1337–1340. [CrossRef]
19. Chen, L.; Chen, Z.; Chen, D.; Xiong, W. Removal of hexalent chromium from contaminated waters by ultrasound-assisted aqueous solution ball milling. *J. Environ. Sci.* **2016**, *52*, 276–283. [CrossRef]
20. Fu, D.; Ma, X.; Chen, D. Degradation of azo dye in wastewater by ultrasonic assisted ball milling. *J. Hunan Univ.* **2017**, *44*, 82–89.
21. Hen, Z.; Zhang, D.-Q.; Wu, Q.; Zheng, X.-H. Improvement on the coupling method for rock ultrasonic probe to a test piece. *J. Liao. Shi. Uni.* **2017**, *37*, 51–54.
22. Yasui, T.K.; Kozuka, T.; Tuziuti, T. Effect of ultrasound pretreatment on the hydrothermal synthesis of SSZ-13 zeolite. *Ultrason. Sonochemistry* **2007**, *14*, 605–612. [CrossRef]
23. Liu, L.; Wen, J.; Yang, Y.; Tan, W. Ultrasound field distribution and ultrasonic oxidation desulfurization efficiency. *Ultrason. Sonochemistry* **2013**, *20*, 696–702. [CrossRef]
24. Gao, J.J.; Xu, K.H.; Hu, J.X.; Huang, H.; Tang, B. Determination of trace hydroxyl radicals by flow injection spectrofluorometry and its analytical application. *J. Agric. Food Chem.* **2006**, *54*, 7968–7972. [CrossRef]
25. Tichenor, L.B.; Graham, J.L.; Yamada, T.; Taylor, P.H.; Peng, J.; Hu, X.; Marshall, P. Kinetic and modeling studies of the reaction of hydroxyl radicals with tetrachloroethylene. *J. Phys. Chem. A* **2000**, *104*, 1700–1707. [CrossRef]
26. Tiehm, A.; Nickel, K.; Zellhorn, M.; Neis, U. Ultrasonic waste activated sludge disintegration for improving anaerobic stabilization. *Waste Res.* **2001**, *35*, 2003–2008. [CrossRef]
27. Mark, G.; Tauber, A.; Laupert, R.; Schuchmann, H.P.; Schulz, D.; Mues, A.; von Sonntag, C. OH-radical formation by ultrasound in aqueous solution-part II: Terephthalate and the sonolytic yield. *Ultrason. Sonochemistry* **1998**, *5*, 41–52. [CrossRef]
28. Wang, X.; Ren, X.; Nian, J.; Li, X. Preparation of photocatalyst at low temperature and its photocatalytic and magnetic recovery properties. *Environ. Sci.* **2020**, *33*, 2752–2758.